Original Article

Iranian Journal of Immunology

March 2026; 23(1):

BATF Drives Cervical Cancer Progression and Immune Evasion by Regulating the STAT1-PD-L1 Axis

Jun Zhang, Yang Zhang*, Jinwei Zhang*

Department of Gynecology, The Affliated Wuxi People's Hospital of Nanjing Medical University, Wuxi Medical Center, NanjingMedical University, Wuxi People'sHospital, Wuxi, Jiangsu 214023, China

ABSTRACT

Background: Cervical cancer progression is driven in part by immune evasion mechanisms, including PD-L1-mediated suppression of T cell activity. BATF, a transcription factor involved in immune regulation, has been implicated in tumor immunity; however, its role in cervical cancer remains incompletely understood.

Objectives: To investigate the role of the BATF-STAT1-PD-L1 axis in tumor progression and immune regulation.

Methods: BATF expression was evaluated in cervical cancer tissues and cell lines. Functional assays performed to assess the effects of BATF knockdown on cell proliferation, apoptosis, autophagy, and migration. Regulation of STAT1 was examined using chromatin immunoprecipitation and Western blot analysis. PD-L1 expression was measured by flow cytometry. In vivo xenograft models were used to evaluate tumor growth and response to PD-L1 blockade.

Results: BATF was upregulated in cervical cancer tissues and cell lines and was associated with enhanced tumor growth, metastasis, and immune evasion. BATF knockdown inhibited cell proliferation, promoted apoptosis and autophagy, and reduced migratory capacity. Mechanistically, BATF transcriptionally activated STAT1, leading to increased PD-L1 expression. BATF suppression enhanced $CD8^+$ T cell infiltration and improved PD-L1 blockade efficacy in vivo. Results: BATF was upregulated in cervical cancer tissues and cell lines and was associated with enhanced tumor growth, metastasis, and immune evasion. BATF knockdown inhibited cell proliferation, promoted apoptosis and autophagy, and reduced migratory capacity. Mechanistically, BATF transcriptionally activated STAT1, leading to increased PD-L1 expression. In vivo, BATF suppression enhanced $CD8^+$ T-cell infiltration and improved the therapeutic efficacy of PD-L1 blockade.

Conclusion: BATF promotes cervical cancer progression by modulating STAT1 and PD-L1. Targeting BATF may enhance anti-tumor immunity and improve immunotherapy outcomes.

Keywords: BATF; STAT1; PD-L1; Cervical cancer; Immune evasion; Checkpoint blockade

*Corresponding author:
Yang Zhang,
Jinwei Zhang,
Department of Gynecology, The Affliated Wuxi People's Hospital of Nanjing Medical University, Wuxi Medical Center, Nanjing Medical University, Wuxi People's Hospital, No. 299 Qingyang Road, Wuxi, Jiangsu 214023, China
Email: zhangyang_edu@outlook.com
Email: Zhangjinwei_666@163.com

Cite this article as:
Zhang J, Zhang Y, Zhang J. BATF Drives Cervical Cancer Progression and Immune Evasion by Regulating the STAT1-PD-L1 Axis. *Iran J Immunol.* 2026; 23(1): ,
doi: .

Received:
Revised:
Accepted:

INTRODUCTION

Cervical cancer remains one of the most prevalent and lethal malignancies among women worldwide. Persistent infection by high-risk human papillomaviruses (HPV) is a primary etiological factor for cervical cancer (1-3). According to WHO data in 2023 (*WHO Fact Sheet: Cervical Cancer*), cervical cancer accounts for approximately 604,000 new cases and 342,000 deaths annually, ranking as the fourth most common malignancy in women worldwide. Despite advancements in screening programs and vaccination, many patients are diagnosed at advanced stages, where treatment options are limited, and prognosis remains poor (4, 5). One of the key steps in cervical cancer progression is immune evasion, which allows tumor cells to escape host immune surveillance and continue malignant proliferation (6, 7). Immune checkpoint pathways such as the programmed death-ligand 1 (PD-L1) axis have been identified as central players in suppressing anti-tumor immunity and facilitating tumor progression (8-10). However, the upstream transcriptional regulators of PD-L1 in cervical cancer remain incompletely understood.

The transcription factor BATF (Basic Leucine Zipper Transcription Factor) is known for its role in immune cell differentiation and tumorigenesis (11-13). Initially recognized as a regulator of T cell exhaustion and immunosuppression, BATF has been implicated in modulating tumor microenvironments by influencing cytokine secretion and immune checkpoint expression (14-16). Recent studies have linked BATF to various cancers, including lung and colorectal cancer, where it contributes to tumor proliferation and immune evasion (17-19). Analysis of TCGA-CESC dataset revealed BATF overexpression in 68% of squamous cell carcinomas (n=255), with higher levels correlating with advanced FIGO stage. However, its precise role in cervical cancer and regulating PD-L1 remains unclear.

STAT1 (Signal Transducer and Activator of Transcription 1) is a crucial mediator of interferon signaling, which plays a complex role in both tumor suppression and immune modulation (20, 21). STAT1 activation is typically associated with enhanced immune responses, however, recent evidence suggests that it can also promote immune evasion by upregulating PD-L1 expression in tumor cells (22). Previous studies in lung adenocarcinoma suggest that BATF directly binds to AP-1 motifs in the STAT1 promoter (23). Although cervical cancer-specific data are limited, our preliminary bioinformatics analysis of TCGA-CESC data revealed a positive correlation between BATF and STAT1 expression ($r=0.41$, $P<0.001$; supplementary Fig. 1A). The interaction between BATF and STAT1 remains incompletely understood, particularly in cervical cancer. Given that both transcription factors are involved in immune regulation and tumor progression, their potential interaction in driving PD-L1 expression warrants further investigation.

Immune checkpoint blockade therapies targeting PD-1/PD-L1 have demonstrated promising results in cervical cancer therapy. However, many of the patients experience either primary or acquired resistance (24, 25). Understanding the molecular mechanisms that regulate PD-L1 expression could provide insights to enhance the efficacy of immunotherapeutic strategies. Given the emerging evidence of the role of BATF and STAT1 in immune regulation, we hypothesized that BATF may act as an upstream regulator of STAT1, contributing to PD-L1-mediated immune evasion in cervical cancer. This study aims to investigate the regulatory role of BATF-STAT1-PD-L1 axis and its impact on cervical cancer progression, tumor proliferation, apoptosis, and autophagy. By uncovering these interactions, we hope to provide new insights into potential therapeutic targets for improving immune-based treatments.

MATERIALS AND METHODS

Cell Culture and Transfection

SiHa, Caski, C33A, and the normal human keratinocyte cell line (HaCaT) were purchased from ATCC (USA). Cells were cultured in DMEM (11885-092, Gibco, USA) at 37°C in a humidified incubator with 5% CO_2. For BATF knockdown, cells were transfected with 50 nM BATF-specific shRNA (sh-BATF: TRCN0000421943) or non-targeting control (sh-NC: SHC002) using Lipofectamine 3000 (L3000015, Invitrogen, USA) following the manufacturer's instructions. Transfection efficiency was assessed 48 hours post-transfection. Transfection efficiency was validated by: (1) Co-transfection with GFP-expressing vector (pEGFP-N1), with >80% fluorescence observed at 24 h; (2) quantifying BATF mRNA using qPCR (>70% reduction vs. sh-NC).

qRT-PCR Analysis

Total RNA was purified using the TRIzol reagent (15596026, Invitrogen, USA) and cDNA was synthesized with the PrimeScript RT reagent kit (RR037A, Takara, Japan). Quantitative real-time PCR (qRT-PCR) was subsequently carried out using SYBR Green Master Mix (A25742, Applied Biosystems, USA) on a QuantStudio 6 Flex Real-Time PCR System (Applied Biosystems, USA) with the following parameters: 95°C for 30 s, 40 cycles of 95°C for 5 s and 60°C for 30 s. Primer sequences (Supplementary Table S1) were designed using NCBI Primer-BLAST and validated by melt curve analysis. GAPDH served as a reference gene (geometric mean normalization). The relative expressions of BATF, STAT1, PD-L1, and immune-related genes were calculated.

Western Blot Analysis

Cells were lysed in RIPA buffer (89900, Thermo Fisher, USA) supplemented with protease and phosphatase inhibitors (78440, Thermo Fisher, USA). Proteins were transferred, membranes were blocked and incubated with primary antibodies targeting BATF (sc-393365, Santa Cruz Biotechnology, USA), STAT1 (9172, Cell Sig, USA), PD-L1 (13684, Cell Sig, USA), Beclin1 (ab207612, Abcam, UK), LC3-II (2775, Cell Sig, USA), P62 (5114, Cell Sig, USA), and GAPDH (60004-1-Ig, Proteintech, USA). After incubating with secondary antibody, bands were analyzed using the ECL detection system.

Flow Cytometry Analysis of PD-L1 Expression

Cells were harvested and stained with PE-conjugated anti-human PD-L1 antibody (329708, BioLegend, USA) at 4°C for 30 minutes in the dark. Flow cytometry was conducted using a BD LSRFortessa system (BD Biosciences, USA).

ELISA for Cytokine Detection

Cytokine levels (CXCL10, CXCL11, CCL5, IFNβ) were measured in cell culture supernatants collected at 48 h post-transfection using commercial ELISA kits (CXCL10: DSA00, R&D Systems, USA; CXCL11: DCX110, R&D Systems, USA; CCL5: DRN00B, R&D Systems, USA; IFNβ: 41435, PBL Assay Science, USA) following the manufacturer's protocols. Medium was replaced with serum-free DMEM 6 h before supernatant collection to avoid FBS interference. Absorbance was measured at 450 nm using a SpectraMax iD3 Microplate Reader (Molecular Devices, USA).

Colony Formation and Cell Viability Assays

For colony formation assays, transfected cells were seeded in 6-well plates at 500 cells / well and maintained for 14 days. After fixation with 4% paraformaldehyde and staining with 0.5% crystal violet, colonies containing more than 50 cells were manually counted under a light microscope (10× magnification). Three independent wells were analyzed per group. CCK-8 assay (96992, Sigma-Aldrich, USA) was used for assessing viability. 5×10^3 cells per well were plated in 96-well plates, treated with CCK-8 reagent for 2 hours, and subsequently, absorbance was measured at 450 nm.

EdU Proliferation Assay

Reagents were accessed from. Transfected cells were exposed to 50 μM EdU (EdU assay kit, C10310, Beyotime, China) for 2 hours, followed by fixation with 4% paraformaldehyde and staining according to the manufacturer's instructions. Nuclei were stained with DAPI, and imaging was performed using a microscope (LSM 880, Zeiss, Germany).

Apoptosis Analysis by Flow Cytometry and TUNEL Assay

Apoptosis was quantified using the Annexin V-FITC/PI apoptosis detection kit (556547, BD Biosciences, USA). Cells were stained according to the manufacturer's protocol and analyzed by flow cytometry. The One-Step TUNEL Apoptosis Assay Kit (C1088, Beyotime, China) was utilized to conduct TUNEL staining. Cells were fixed, permeabilized, and stained as instructed. Fluorescence outcomes were visualized using a fluorescence microscope (Axio Observer 7, Zeiss, Germany).

Transwell Migration and Invasion Assays

In migration assays, 2×10^5 cells were placed in the upper compartment of Transwell inserts with 8-μm pores in a serum-free medium. For invasion assays, the inserts were first layered with Matrigel. After a 24-hour incubation, cells that migrated were stained with crystal violet, and observed under a light microscope.

Wound Healing Assay

Upon 90% confluence of cell growth, a scratch was introduced with a sterile pipette tip. The medium was then replaced with serum-free DMEM. Wound width was measured at three fixed points in each well using ImageJ v1.53 (NIH). Migration rate (%) = $[(Width_{0\,h} - Width_{24\,h})/Width_{0\,h}] \times 100\%$.

Chromatin Immunoprecipitation (ChIP) Assay

SimpleChIP Plus Kit (9005, Cell Signaling Technology, USA) was used. ChIP assays targeted the STAT1 promoter region (chr2:190, 863, 402-190, 863, 902, hg38), including a predicted AP-1 binding site at -320 bp (positive control). IgG and input DNA served as controls. Primers spanning -500 to +100 bp relative to TSS (supplementary Table S2). Cells were crosslinked with 1% formaldehyde, lysed, and sonicated using a Bioruptor (Diagenode, Belgium). Immunoprecipitation was performed with anti-BATF (sc-393365, Santa Cruz Biotechnology, USA) or IgG control. DNA was purified and analyzed by qRT-PCR.

In Vivo Xenograft and Lung Metastasis Models

BALB/c nude mice, aged six weeks, were obtained from Charles River in China. In the xenograft model, 5×10^6 sh-NC or sh-BATF-transfected Caski cells were subcutaneously implanted in the flank, and tumor volume was recorded every 4 days. Mice were euthanized on day 28, and tumors were excised and weighed. In the lung metastasis model, 1×10^6 transfected cells were infused via the tail vein. After 6 weeks, lung metastases were evaluated using micro-CT scanning, followed by histological examination of the dissected lung tissues.

Immunohistochemistry (IHC) Staining

Paraffin-embedded tumor sections were stained with antibodies against Ki-67 (ab15580, Abcam, UK), PCNA (ab92552, Abcam, UK), LC3B (ab192890, Abcam, UK), and PD-L1 (13684, Cell Signaling Technology, USA). After secondary antibody incubation, results were visualized using DAB substrate. Images were acquired using an Olympus BX53 microscope (Olympus, Japan).

Statistical Analysis

All functional assays (proliferation, apoptosis, migration) included 3 biological replicates (independent cell cultures/passages); 2 technical repeats per replicate. However, RNA/protein extraction included 3 biological replicates without technical

repeats) and animal studies included 8 mice/group with no technical repeats). Results are reported as the mean with standard deviation (SD). Statistical comparisons among groups were carried out using either Student's *t*-test or one-way ANOVA, with significance established at $P < 0.05$. Data processing was conducted using GraphPad Prism 9 (GraphPad Software, USA).

RESULTS

BATF Was Upregulated in Cervical Cancer

Bioinformatics analysis using the GEPIA database revealed that BATF expression was pronouncedly elevated in cervical cancer tissues relative to normal ones, indicating a potential oncogenic role in cervical cancer (Fig. 1A). qRT-PCR confirmed that BATF level was markedly higher in cervical cancer tissues (Fig. 1B). Consistently, BATF mRNA levels were also elevated in Caski, C33A, and SiHa cell lines, relative to the normal human keratinocyte cell line HaCaT, suggesting its widespread overexpression (Fig. 1C). To investigate the functional role of BATF, shRNA-mediated knockdown was conducted in Caski and C33A cells, which were selected due to their relatively high BATF expression. Previous evidence showed that UBE2C is transcriptionally regulated by BATF in gynecologic cancers, therefore, we first validated BATF knockdown efficiency, then assessed UBE2C expression. qRT-PCR analysis confirmed a substantial loss in BATF mRNA levels upon transfection with sh-BATF relative to the control group, indicating effective knockdown at the transcript level (Fig. 1D). Furthermore, Western blot analysis demonstrated a significant decrease in BATF protein levels following sh-BATF transfection in both cell lines, further confirming the knockdown efficiency at the protein level (Fig. 1E, F). These results collectively indicate that BATF is highly expressed in cervical cancer and can be effectively silenced through shRNA-mediated knockdown.

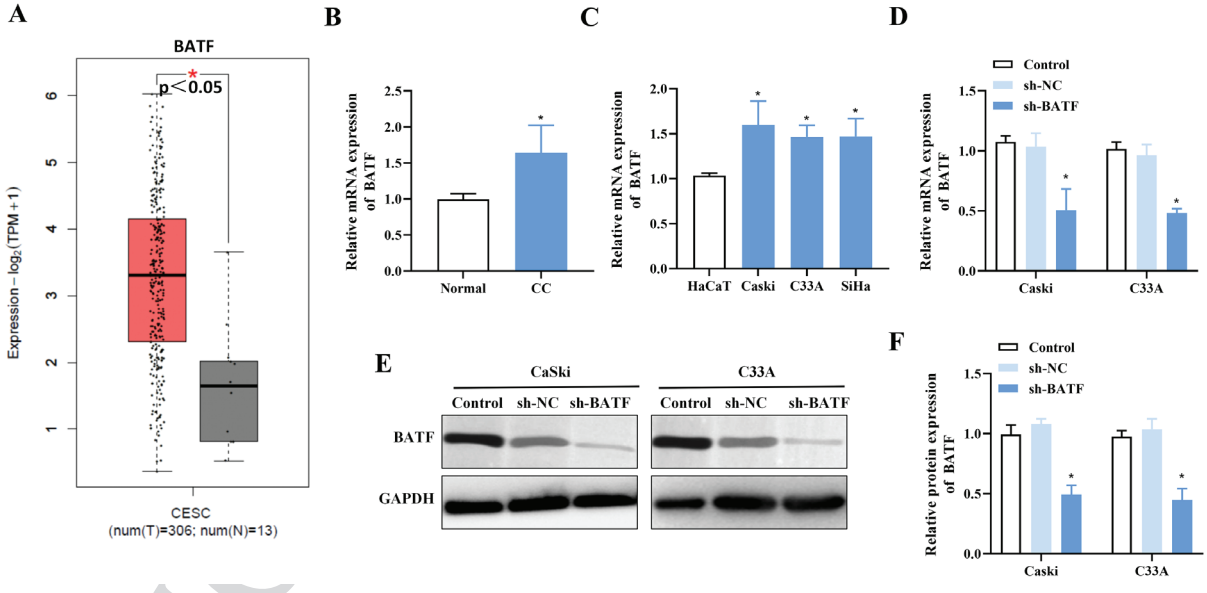

Fig. 1. Analysis of BATF expression in cervical cancer. (A) GEPIA database analysis of BATF expression in cervical cancer cells. (B) qRT-PCR analysis of BATF expression in cervical cancer and adjacent normal tissues. Gene expressions were normalized to GAPDH and β-actin. Primer sequences are presented in Table S1. (C) qRT-PCR analysis of BATF expression in cervical cancer cell lines. Gene expressions were normalized to GAPDH and β-actin. Primer sequences are presented in Table S1. (D) qRT-PCR validation of BATF knockdown efficiency in cervical cancer cell lines. Transfection efficiency was >80% in GFP control group, with BATF mRNA reduced by 72±5% in sh-BATF-1 and 68±4% in sh-BATF-2. (E) Western blot analysis of BATF protein expression after knockdown. (F) Densitometric analysis of Western blot results for BATF knockdown. Data represent mean±SD of 3 biological replicates with 2 technical repeats/assay. *P<0.05, **P<0.01, ***P<0.001 (two-tailed Student's t-test or ANOVA with Tukey's post-hoc).

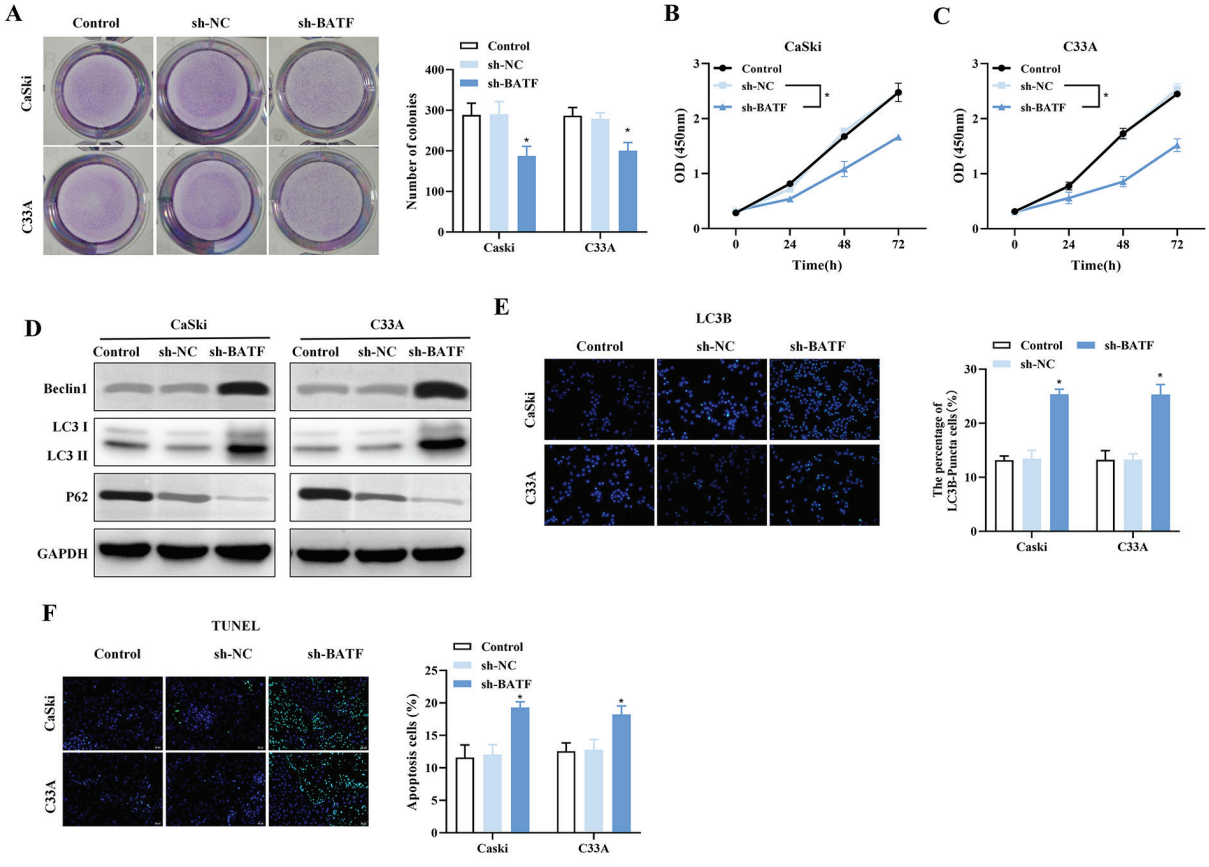

Fig. 2. BATF knockdown impacts cell proliferation, autophagy, and apoptosis. (A) Colony formation assay for evaluating cervical cancer cell proliferation. (B) Viability of cervical cancer cells was determined using CCK-8 assay. (C) Time-course CCK-8 assay for examining cervical cancer cell viability. (D) Western blot analysis of Beclin1, LC3-II, and P62 protein expression. (E) Immunofluorescence staining of LC3B-positive cells. (F) TUNEL staining of apoptotic cells. Data represent mean±SD of 3 biological replicates with 2 technical repeats/assay. *P<0.05, **P<0.01, ***P<0.001 (two-tailed Student's t-test or ANOVA with Tukey's post-hoc).

BATF Knockdown Promoted Autophagy and Apoptosis in Cervical Cancer Cells

The number of colonies was reduced in the sh-BATF group relative to the sh-NC and control groups, indicating that BATF knockdown suppressed the proliferative capacity of cervical cancer cells (Fig. 2A). Similarly, CCK-8 assays showed that cell viability was significantly decreased in the sh-BATF group at multiple time points, further confirming the inhibitory effect of BATF knockdown on cell growth (Fig. 2B, C). Given the role of autophagy in cancer progression, Western blot analysis was conducted to examine the expression of key autophagy-related proteins. The results demonstrated that Beclin1 and LC3-II protein levels were elevated, whereas P62 expression was markedly reduced in the sh-BATF group relative to controls, suggesting enhanced autophagic activity following BATF silencing (Fig. 2D). Consistently, immunofluorescence staining demonstrated a significant increase in LC3B-positive puncta in sh-BATF-transfected cells, further confirming the induction of autophagy (Fig. 2E). In addition, TUNEL staining demonstrated a substantial increase in apoptotic cells in the sh-BATF group (Fig. 2F). These findings collectively indicate that BATF suppression enhances both autophagy and apoptosis, contributing to the inhibition of cervical cancer cell proliferation.

BATF Knockdown Inhibited the Migration and Invasion of Cervical Cancer Cells

To evaluate the effect of BATF knockdown on cervical cancer cell motility, mobility

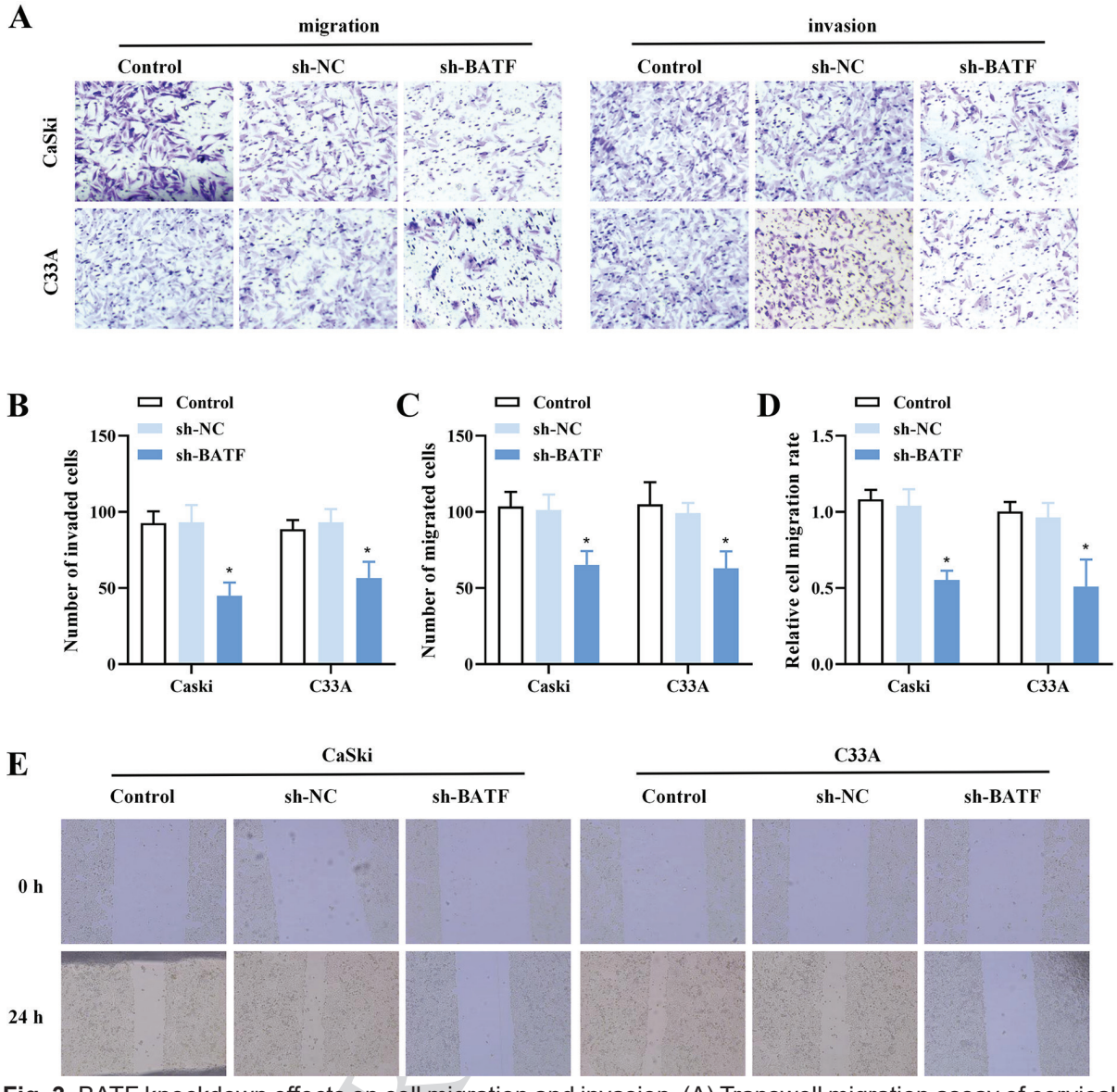

Fig. 3. BATF knockdown effects on cell migration and invasion. (A) Transwell migration assay of cervical cancer cells. (B) Quantification of migrated cells in the Transwell assay. (C) Transwell invasion assay of cervical cancer cells. (D) Wound healing assay for evaluating cervical cancer cell migration. (E) Quantification of wound closure in the wound healing assay. Data represent mean±SD of 3 biological replicates with 2 technical repeats/assay. *P<0.05, **P<0.01, ***P<0.001 (two-tailed Student's t-test or ANOVA with Tukey's post-hoc).

assays were performed. The number of migrated and invaded cells was significantly lower in the sh-BATF group, indicating that BATF knockdown markedly suppressed both migratory and invasive abilities of tumor cells (Fig. 3A-C). Consistently, wound healing assays demonstrated a significant decline in wound closure rates in the sh-BATF group, further verifying the inhibitory effect of BATF silencing on cell migration (Fig. 3D-E). These findings suggest that BATF promotes cervical cancer cell motility, and its knockdown effectively impairs migration and invasion.

BATF Knockdown Increased the Expression of Immune-related Cytokines and Interferon-stimulated Genes

To investigate the effect of BATF knockdown on the expression of immune-related genes, qRT-PCR was conducted and to assess the transcript levels of multiple cytokines and interferon-stimulated genes (ISGs). The results demonstrated that the

expression levels of CXCL11, CCL5, IFNB, IFIT2, IFIT3, OASL, TNF, IFITM1, IFITM3, IFI27, IFI16, Noxa, RIG-1, IFI44, and IRF7 were upregulated in the sh-BATF group, indicating the activation of the immune response upon BATF silencing (Fig. 4A). Additionally, ELISA results confirmed a significant increase in CXCL10 protein levels in the sh-BATF group, while BATF overexpression led to a significant decrease in its secretion, verifying that BATF negatively regulates CXCL10 expression (Fig. 4B). Similarly, CXCL11 and CCL5 levels were higher in the sh-BATF group and lower in the BATF-overexpressing group, further supporting the role of BATF in suppressing chemokine production (Fig. 4C, D). Moreover, IFNβ secretion was elevated following BATF knockdown, whereas its levels were pronouncedly reduced upon BATF overexpression, indicating that BATF negatively regulates interferon production (Fig. 4E). These findings suggest that BATF functions as a repressor of immune-related cytokines and ISGs, and its knockdown enhances the immune-related pathways in cervical cancer cells.

BATF Regulates PD-L1 Expression through STAT1 in Cervical Cancer Cells

Analysis revealed a significant positive correlation between BATF and STAT1 expression, suggesting a regulatory relationship between these two factors (Fig. 5A). Relative to the control vector group, BATF overexpression increased PD-L1 expression, whereas treatment with the STAT1 inhibitor Fludarabine attenuated this effect (Fig. 5B-D). Correspondingly, western blot analysis demonstrated that STAT1 protein levels were significantly decreased in both sh-BATF-1- and sh-BATF-2 -transfected cells, indicating that BATF positively regulates STAT1 expression (Fig. 5E-G).

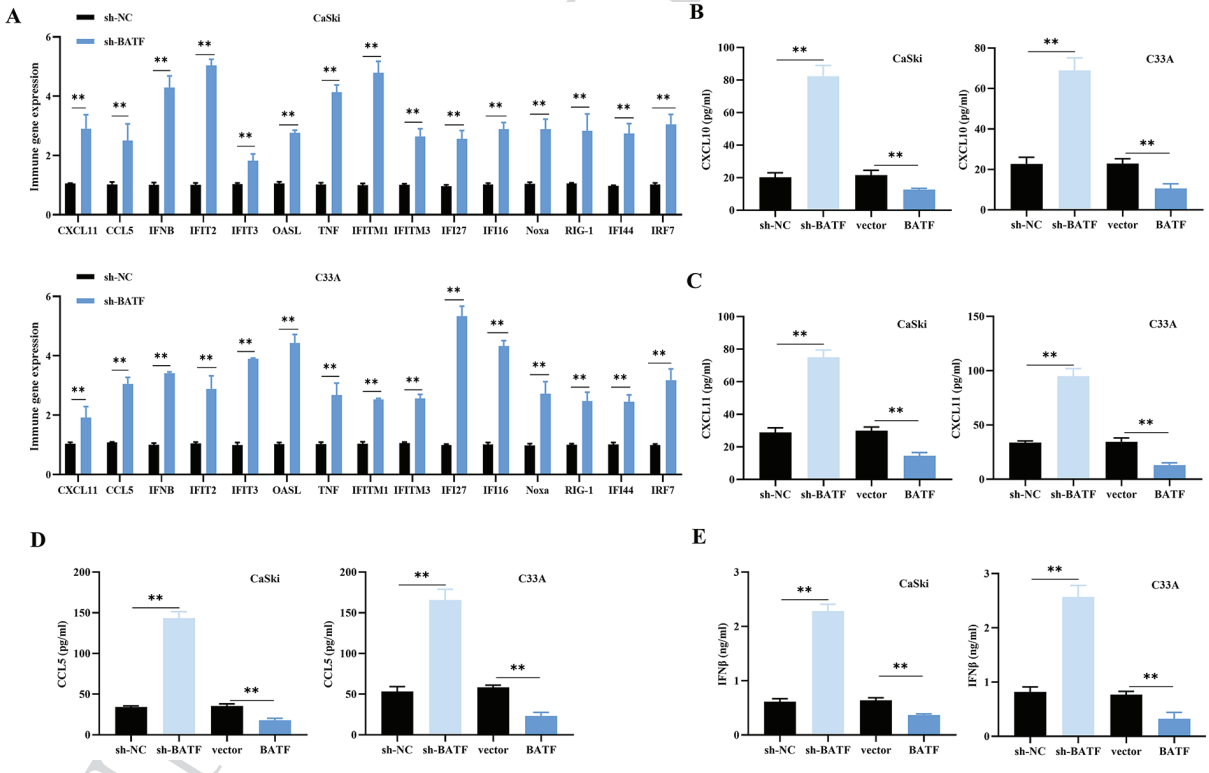

Fig. 4. BATF knockdown impacts immune-related gene expression. (A) qRT-PCR analysis of the expression of immune-related genes in cervical cancer cells. Gene expressions were normalized to GAPDH and β-actin. Primer sequences were presented in Table S1. (B) ELISA analysis of CXCL10 protein levels. (C) ELISA analysis of CXCL11 protein levels. (D) ELISA analysis of CCL5 protein levels. (E) ELISA analysis of IFNβ protein levels. Data represent mean±SD of 3 biological replicates with 2 technical repeats/assay. *P<0.05, **P<0.01, ***P<0.001 (two-tailed Student's t-test or ANOVA with Tukey's post-hoc).

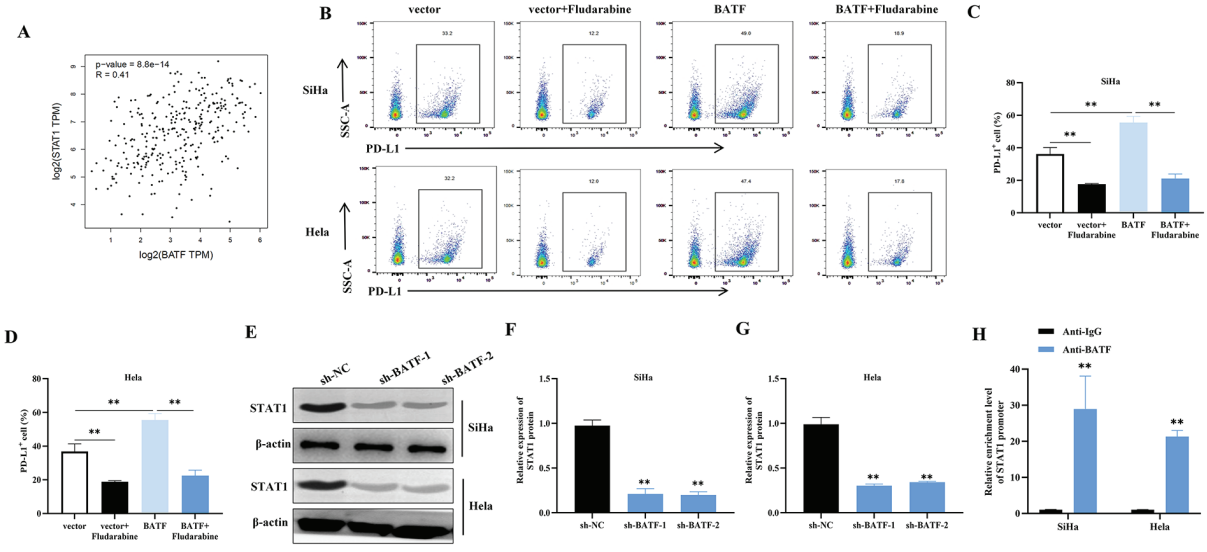

Fig. 5. BATF regulates PD-L1 expression through STAT1. (A) Correlation analysis of BATF and STAT1 expression. (B) Flow cytometry assessment of PD-L1 expression after BATF modulation. (C) Analysis of PD-L1 expression by flow cytometry. (D) Flow cytometry analysis of the effect of Fludarabine treatment on PD-L1 expression. (E) Western blot analysis of STAT1 protein expression after BATF knockdown. (F) Densitometric analysis of Western blot results for STAT1. (G) Western blot analysis of STAT1 protein expression across different knockdown groups. (H) ChIP assay of the BATF binding to the STAT1 promoter. ChIP-qPCR showing BATF enrichment at STAT1 promoter AP-1 site vs. IgG. Negative control: intergenic region. Data represent mean±SD of 3 biological replicates with 2 technical repeats/assay. *P<0.05, **P<0.01, ***P<0.001 (two-tailed Student's t-test or ANOVA with Tukey's post-hoc).

Furthermore, chromatin immunoprecipitation (ChIP) assays revealed a significant BATF enrichment in the STAT1 promoter region, as indicated by increased DNA binding in the anti-BATF group relative to the IgG control, verifying direct transcriptional regulation of STAT1 by BATF (Fig. 5H). These findings suggest that BATF modulates PD-L1 expression in cervical cancer by transcriptionally activating STAT1, a key mediator in immune regulation.

BATF Impacts Cervical Cancer Cell Growth, Programmed Cell Death, and Autophagic Activity Via STAT1

To investigate whether STAT1 mediates the effects of BATF in cervical cancer cells, STAT1 was overexpressed in BATF-silenced cells (Fig. 6A). EdU incorporation assays demonstrated a significant decrease in cell proliferation in the sh-BATF+vector group, while STAT1 overexpression partially counteracted this effect, indicating that BATF promotes cervical cancer cell proliferation through STAT1 (Fig. 6B). Similarly, flow cytometry analysis demonstrated that apoptosis was increased in the sh-BATF+vector group, whereas STAT1 overexpression reversed this trend, indicating that BATF inhibits apoptosis via STAT1 (Fig. 6C, E). Given the observed effects of BATF on autophagy, Western blot analysis was performed to assess key autophagy-related proteins. Beclin1 and LC3-II levels were markedly increased, while P62 expression was reduced following BATF knockdown, indicating enhanced autophagic activity. However, STAT1 overexpression attenuated these effects, restoring P62 expression while reducing Beclin1 and LC3-II levels (Fig. 6D). Consistently, immunofluorescence staining showed a significant increase in LC3B-positive puncta in the sh-BATF+vector group, which was partially reversed upon STAT1 overexpression, further confirming the role of BATF in autophagy regulation via STAT1 (Fig. 6F-G). These findings collectively suggest that BATF modulates cervical cancer cell proliferation, apoptosis, and autophagy through STAT1.

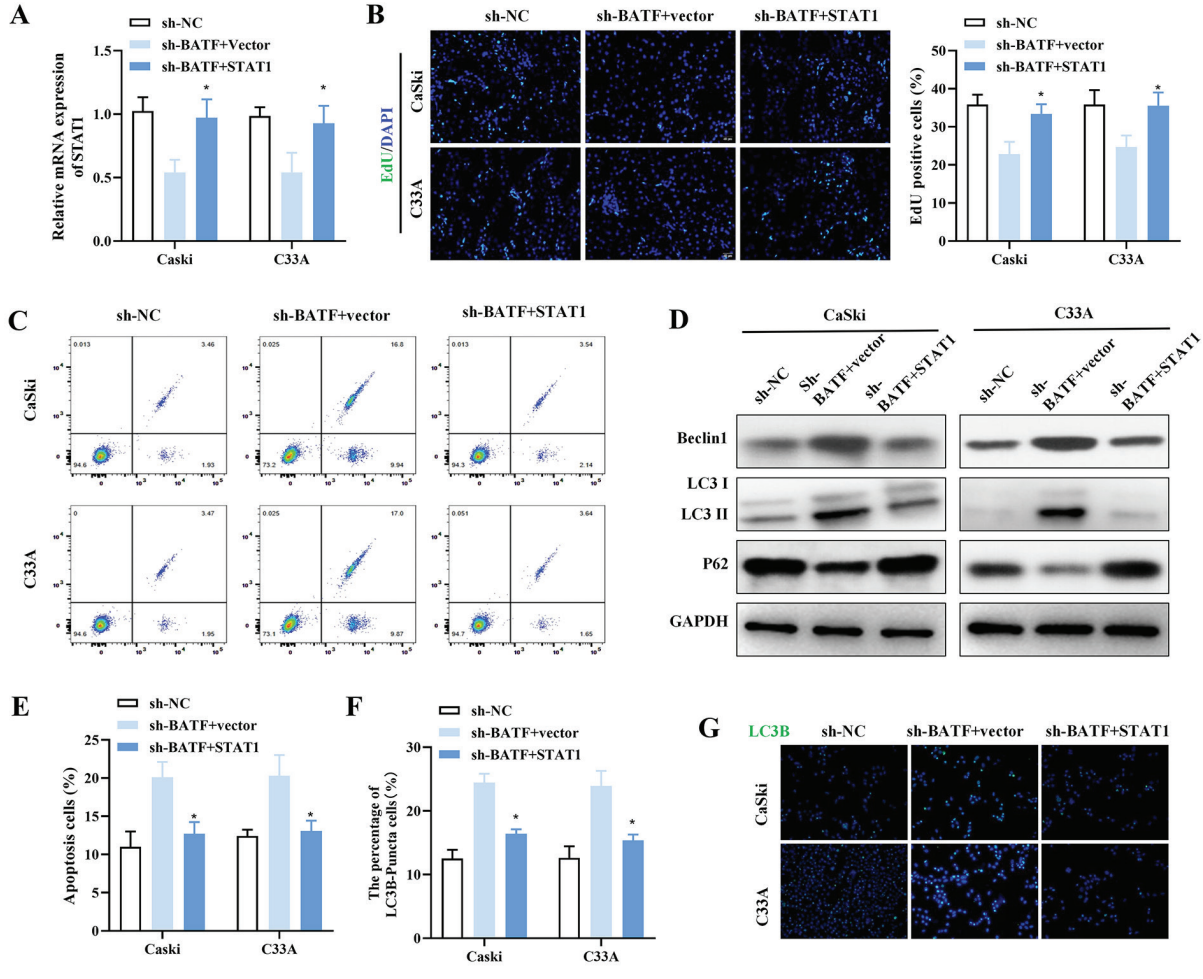

Fig. 6. BATF-STAT1 regulation of cell proliferation, apoptosis, and autophagy. (A) Schematic representation of the STAT1 overexpression in BATF knockdown cells. (B) Assessment of the cell proliferation using EdU assay. (C) Flow cytometry analysis of apoptotic cells. (D) Western blot analysis of Beclin1, LC3-II, and P62 protein expression. (E) Quantification of apoptotic cells using flow cytometry. (F) Immunofluorescence staining of LC3B-positive cells. (G) Quantification of LC3B-positive cells by immunofluorescence analysis. Data represent mean±SD of 3 biological replicates with 2 technical repeats/assay. *P<0.05, **P<0.01, ***P<0.001 (two-tailed Student's t-test or ANOVA with Tukey's post-hoc).

BATF Knockdown Suppressed Tumor Growth and Metastasis In Vivo

A xenograft model was established by implanting nude mice with cervical cancer cells transfected with either sh-NC or sh-BATF via subcutaneous injection (Fig. 7A). Tumor growth was inhibited in the sh-BATF group, as evidenced by a significant reduction in both tumor volume and tumor weight (Fig. 7B-C). UBE2C, a downstream target of BATF implicated in cervical cancer metastasis, was downregulated upon BATF silencing. It was verified that UBE2C expression was significantly reduced following BATF silencing, indicating that BATF may regulate tumor progression via UBE2C (Fig. 7D-E). Western blot analysis of apoptosis-related proteins demonstrated increased expression of pro-apoptotic markers in the sh-BATF group, further verifying the induction of apoptosis following BATF silencing (Fig. 7F). Additionally, Western blot analysis of key autophagy-related proteins showed increased expression of Beclin1 and LC3-II, along with decreased P62 levels in sh-BATF tumors, suggesting enhanced autophagic activity (Fig. 7G). Immunohistochemical (IHC) staining of tumor tissues demonstrated downregulated proliferation markers in the sh-BATF group, while LC3 was upregulated,

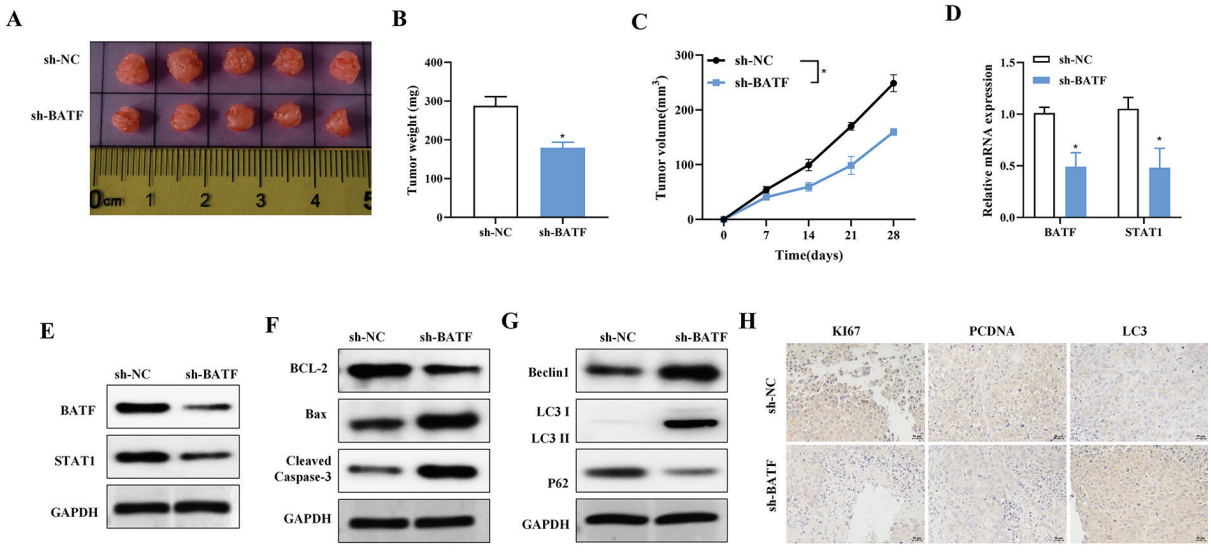

Fig. 7. Effects of BATF knockdown on tumor growth and metastasis in vivo. (A) Xenograft tumor model of cervical cancer using tumor cells transfected with sh-NC or sh-BATF. (B) Measurement of the tumor volume in xenograft models. (C) Tumor weight measurement in xenograft models. (D) qRT-PCR analysis of UBE2C expression after BATF knockdown. (E) Western blot analysis of UBE2C protein expression after BATF knockdown. (F) Western blot analysis of apoptosis-related proteins. (G) Western blot analysis of Beclin1, LC3-II, and P62 protein expression. (H) Immunohistochemistry staining of Ki-67, PCNA, and LC3 in tumor tissues. Data represent mean±SD of 3 biological replicates with 2 technical repeats/assay. *P<0.05, **P<0.01, ***P<0.001 (two-tailed Student's t-test or ANOVA with Tukey's post-hoc).

further supporting the role of BATF in tumor cell proliferation and autophagy regulation (Fig. 7H). These results collectively suggest that BATF knockdown suppresses tumor growth and metastasis by modulating apoptosis, autophagy, and proliferation in cervical cancer cells.

Silencing BATF Increased the Effecacy of PD-L1 Inhibition in Immunotherapy

To investigate the effect of BATF knockdown on the immune response against tumor, and its interaction with PD-L1 blockade, cervical cancer cells transfected with either sh-NC or sh-BATF were implanted in mice, followed by anti-PD-L1 treatment. Tumor size was reduced in bothsh-BATF and anti-PD-L1 groups, and the combination of BATF knockdown and anti-PD-L1 therapy further suppressed tumor growth, suggesting a synergistic effect (Fig. 8A). Tumor weight significantly decreased in the sh-BATF and anti-PD-L1 groups, with maximum reduction observed in the combination group, further supporting the enhanced therapeutic effect of BATF silencing in combination with PD-L1 blockade (Fig. 8B). Tumor volume measurements further demonstrated a significant reduction in tumor growth across all treatment groups, with the combination therapy displaying the greatest inhibitory effect (Fig. 8C). Western blot confirmed that PD-L1 level markedly decreased in the sh-BATF group, indicating that BATF knockdown negatively regulated PD-L1 level at the protein level (Fig. 8D). Flow cytometry demonstrated that the proportions of $CD45^+CD3^+$, $CD45^+CD3^+CD4^+$, and $CD45^+CD3^+CD8^+$ T cells were increased in the sh-BATF group, and the effect was more pronounced in sh-BATF group receiving anti-PD-L1 therapy. Notably, the percentage of $CD8^+$ T cells expressing granzyme B (GZMB), a key cytotoxic molecule, was elevated in the sh-BATF group, indicating enhanced cytotoxic capability in T cells (Fig. 8E). Consistently, the percentage of $CD45^+CD3^+CD8^+$ T cells increased following BATF knockdown and was further enhanced by PD-L1 blockade, suggesting an improved anti-tumor immune response (Fig. 8F).

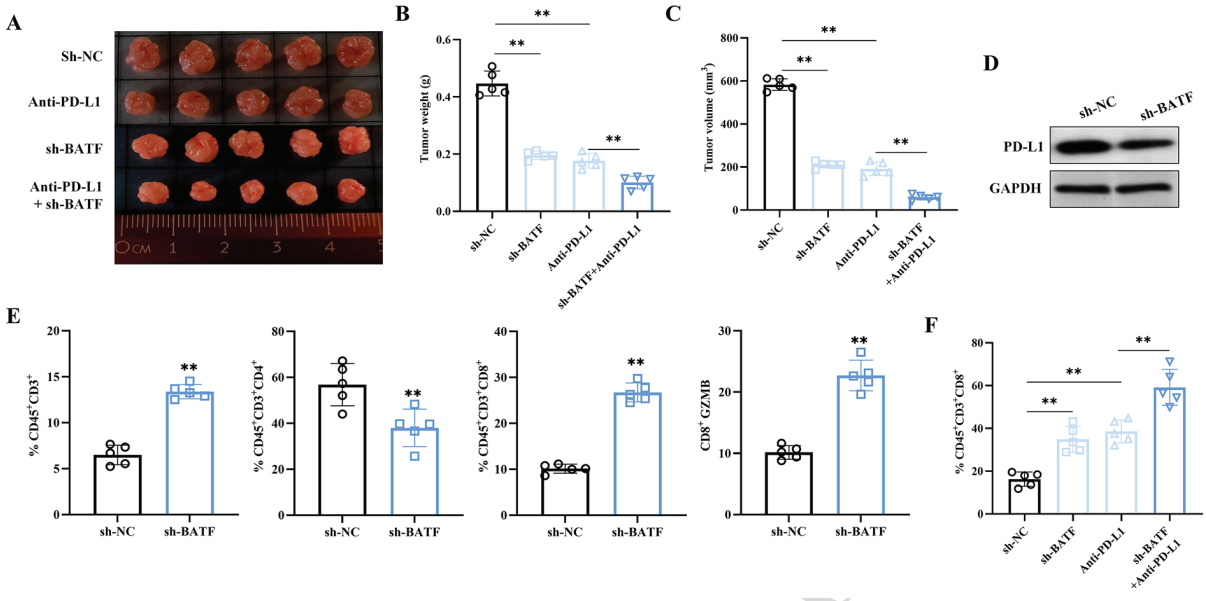

Fig. 8. Effects of the BATF knockdown on PD-L1 blockade. (A) Tumor size measurement in different treatment groups. (B) Tumor weight measurement in different treatment groups. (C) Tumor volume measurement in different treatment groups. (D) Western blot analysis of PD-L1 protein expression. (E) Flow cytometry analysis of T cell subpopulations $CD45^+CD3^+$, $CD45^+CD3^+CD4^+$, $CD45^+CD3^+CD8^+$, $CD8^+GZMB^+$. (F) Flow cytometry analysis of $CD45^+CD3^+CD8^+$ T cells in different treatment groups. Data represent mean±SD of 3 biological replicates with 2 technical repeats/assay. *P<0.05, **P<0.01, ***P<0.001 (two-tailed Student's t-test or ANOVA with Tukey's post-hoc).

These findings collectively indicate that BATF knockdown enhances anti-tumor immunity by promoting T cell infiltration and activation, thereby improving the efficacy of PD-L1 blockade in cervical cancer immunotherapy.

DISCUSSION

The basic leucine zipper transcription factor ATF-like (BATF) belongs to the AP-1 transcription factor family. It is known for its role in immune cell differentiation and tumor progression. BATF has been implicated in multiple cancer types, including cervical cancer, where it modulates various oncogenic processes such as proliferation, apoptosis, autophagy, and immune evasion (26). The present study demonstrated that BATF is highly expressed in cervical cancer tissues and cell lines, and its knockdown suppressed tumor growth and metastasis, at least in part through the STAT1 signaling pathway. Furthermore, BATF silencing enhanced the immune response and sensitized tumors to PD-L1 blockade, suggesting a crucial role for BATF in cervical cancer pathophysiology.

Proliferation and apoptosis are two opposing forces that regulate cancer progression. Our study showed that BATF knockdown inhibited cervical cancer cell proliferation. This result aligns with previous studies that have demonstrated BATF's involvement in tumor cell survival (27). Additionally, the increase in apoptotic cells following BATF depletion, as indicated by TUNEL staining and Western blot analysis of apoptotic markers, suggests that BATF supports cervical cancer cell survival by suppressing apoptosis. A similar role for BATF in regulating apoptosis has been observed in other malignancies, such as hepatocellular carcinoma and breast cancer (28).

Autophagy exhibits a dual role in tumor biology, promoting both survival and cell death-inducing processes based on the cellular context. In this study, BATF knockdown resulted in elevated levels of autophagy-related proteins, such as Beclin1 and LC3-II, while reducing P62 expression, suggesting

that BATF acts as a suppressor of autophagy in cervical cancer cells. Previous research has shown that autophagy suppresses tumor growth by degrading damaged organelles and proteins, thereby reducing tumorigenesis (29, 30). Our findings align with previous studies demonstrating that autophagy activation in cancer cells is frequently associated with decreased proliferation and increased apoptosis (31).

Tumor metastasis remains a major factor contributing to poor prognosis in cervical cancer. In this study, BATF knockdown suppressed both migration and invasion of cervical cancer cells. Similar findings have been reported in colorectal and lung cancers, where BATF enhances epithelial-mesenchymal transition (EMT) and promotes invasive behavior (32, 33). The observed decrease in migration and invasion following BATF knockdown suggests that targeting BATF may be an effective strategy for limiting cervical cancer metastasis.

STAT1 is a critical transcription factor involved in immune response regulation and has been implicated in tumor immune evasion through its role in PD-L1 expression (34, 35). Our results suggest that BATF upregulates STAT1, and ChIP analysis demonstrated that BATF directly binds to the STAT1 promoter. Moreover, Elevated STAT1 expression counteracted the suppressive impact of BATF depletion on cellular proliferation and viability, further supporting its role as a key downstream effector of BATF. These results align with prior studies demonstrating that the BATF-STAT1 axis promotes immune evasion and tumor progression (36-38).

PD-L1-mediated immune evasion is a major challenge in cervical cancer therapy. Our study demonstrated that silencing BATF resulted in a marked decrease in PD-L1 levels, suggesting that BATF contributes to immune evasion by upregulating PD-L1. Flow cytometry analysis demonstrated increased $CD8^+$ T cell infiltration and activation following BATF knockdown, an effect further enhanced when combined with PD-L1 blockade. These findings align with previous reports indicating that the BATF-STAT1-PD-L1 axis plays a crucial role in suppressing anti-tumor immunity (34).

Furthermore, our results demonstrated that BATF knockdown upregulated multiple immune-related genes, including CXCL11, CCL5, IFNB, and IFIT family members, all of which are known to enhance anti-tumor immunity (39). The greatest suppression oftumor growth was observed when BATF depletion was combined with anti-PD-L1 therapy, underscoring the therapeutic potential of BATF inhibition in enhancing the efficacy of the immune checkpoint blockade.

While our findings elucidate the significance of the BATF-STAT1-PD-L1 axis in cervical cancer, several limitations should be considered: 1) Clinical translation gap: results derived solely from cell lines and xenografts should be validated in patient-derived organoids or fresh tumors. 2) HPV status bias: all tested cell lines (SiHa/Caski) are HPV16-positive, limiting generalizability to HPV-negative cases. 3) shRNA specificity: despite scrambled controls, off-target effects cannot be fully excluded andfuture studies should employ CRISPR knockout or rescue experiments. 4) Microenvironment simplification: the in vivo model lacks human immune components, potentially underestimating PD-L1 blockade efficacy.

This study presents strong evidence that BATF is a key regulator of cervical cancer progression by promoting proliferation, inhibiting apoptosis and autophagy, enhancing migration and invasion, and facilitating immune evasion through the STAT1-PD-L1 axis. Knockdown of BATF not only suppressed tumor growth and metastasis but also enhanced anti-tumor immunity and increased sensitivity to PD-L1 blockade. Given the growing interest in immunotherapy for cervical cancer, targeting BATF may represent a promising therapeutic approach to improve treatment outcomes.

The BATF-STAT1-PD-L1 axis may extend beyond cervical cancer: BATF is

overexpressed in HPV+ oropharyngeal cancers, suggesting a viral oncogene linkage. In ovarian cancer, BATF drives IL-10-mediated immunosuppression, whereas STAT1-UBE2C crosstalk has been shown in endometrial cancer. PD-L1 blockade efficacy in different tumor types may depend on BATF expression levels, necessitating biomarker stratification. Due to pan-gynecologic immunosuppressive role of BATF, its targeting may enhance immunotherapy in HPV+ tumors beyond cervical cancer, particularly in BATF-high subsets.

FUNDING

This work was supported by the Wuxi Maternal and Child Health Research Project Major Project (No. FYKY202301).

CONFLICTS OF INTEREST

The authors declare no conflicts of interest.

REFERENCES

1. Johnson CA, James D, Marzan A, Armaos M. Cervical Cancer: An Overview of Pathophysiology and Management. Semin Oncol Nurs. 2019;35(2):166-74.
2. Burd EM. Human papillomavirus and cervical cancer. Clin Microbiol Rev. 2003;16(1):1-17.
3. Buskwofie A, David-West G, Clare CA. A Review of Cervical Cancer: Incidence and Disparities. J Natl Med Assoc. 2020;112(2):229-32.
4. Abu-Rustum NR, Yashar CM, Arend R, Barber E, Bradley K, Brooks R, et al. NCCN Guidelines® Insights: Cervical Cancer, Version 1.2024. J Natl Compr Canc Netw. 2023;21(12):1224-33.
5. Olusola P, Banerjee HN, Philley JV, Dasgupta S. Human Papilloma Virus-Associated Cervical Cancer and Health Disparities. Cells. 2019;8(6).
6. Vanajothi R, Srikanth N, Vijayakumar R, Palanisamy M, Bhavaniramya S, Premkumar K. HPV-mediated Cervical Cancer: A Systematic Review on Immunological Basis, Molecular Biology, and Immune Evasion Mechanisms. Curr Drug Targets. 2022;23(8):782-801.
7. Bonfill-Teixidor E, Neva-Alejo A, Arias A, Cuartas I, Iurlaro R, Planas-Rigol E, et al. Cervical Cancer Evades the Host Immune System through the Inhibition of Type I Interferon and CXCL9 by LIF. Clin Cancer Res. 2024;30(19):4505-16.
8. Xie Y, Kong W, Zhao X, Zhang H, Luo D, Chen S. Immune checkpoint inhibitors in cervical cancer: Current status and research progress. Front Oncol. 2022;12:984896.
9. Han X, Chang WW, Xia X. Immune checkpoint inhibitors in advanced and recurrent/metastatic cervical cancer. Front Oncol. 2022;12:996495.
10. Sharma S, Deep A, Sharma AK. Current Treatment for Cervical Cancer: An Update. Anticancer Agents Med Chem. 2020;20(15):1768-79.
11. Zhang X, Zhang C, Qiao M, Cheng C, Tang N, Lu S, et al. Depletion of BATF in CAR-T cells enhances antitumor activity by inducing resistance against exhaustion and formation of central memory cells. Cancer Cell. 2022;40(11):1407-22.e7.
12. Seo H, González-Avalos E, Zhang W, Ramchandani P, Yang C, Lio CJ, et al. BATF and IRF4 cooperate to counter exhaustion in tumor-infiltrating CAR T cells. Nat Immunol. 2021;22(8):983-95.
13. Itahashi K, Irie T, Yuda J, Kumagai S, Tanegashima T, Lin YT, et al. BATF epigenetically and transcriptionally controls the activation program of regulatory T cells in human tumors. Sci Immunol. 2022;7(76):eabk0957.
14. Fan T, Xiao C, Muhammad S, Li C, He J. BATF reprograms the tumor immune status. Med. 2023;4(1):10-2.
15. Wang X, Hong Y, Zou J, Zhu B, Jiang C, Lu L, et al. The role of BATF in immune cell differentiation and autoimmune diseases. Biomark Res. 2025;13(1):22.
16. Jia C, Ma Y, Wang M, Liu W, Tang F, Chen J. Evidence of Omics, Immune Infiltration, and Pharmacogenomics for BATF in a Pan-Cancer Cohort. Front Mol Biosci. 2022;9:844721.
17. Sorrentino C, D'Antonio L, Fieni C, Ciummo SL, Di Carlo E. Colorectal Cancer-Associated Immune Exhaustion Involves T and B Lymphocytes and Conventional NK Cells and Correlates With a Shorter Overall Survival. Front Immunol. 2021;12:778329.
18. Wang X, Chan S, Dai L, Xu Y, Yang Q, Wang M, et al. Identification of novel T cell proliferation patterns, potential biomarkers and therapeutic drugs in colorectal cancer. J Cancer. 2024;15(5):1234-54.
19. Punkenburg E, Vogler T, Büttner M, Amann K, Waldner M, Atreya R, et al. Batf-dependent Th17 cells critically regulate IL-23 driven colitis-associated colon cancer. Gut. 2016;65(7):1139-50.

20. Clark DN, Begg LR, Filiano AJ. Unique aspects of IFN-γ/STAT1 signaling in neurons. Immunol Rev. 2022;311(1):187-204.
21. Butturini E, Carcereri de Prati A, Mariotto S. Redox Regulation of STAT1 and STAT3 Signaling. Int J Mol Sci. 2020;21(19).
22. Zhang Y, Wang M, Ye L, Shen S, Zhang Y, Qian X, et al. HKDC1 promotes tumor immune evasion in hepatocellular carcinoma by coupling cytoskeleton to STAT1 activation and PD-L1 expression. Nat Commun. 2024;15(1):1314.
23. Liu X, Zhou W, Zheng D, Yang X, Qing Y, Liao W, et al. BATF-Activated AIM2 Mediates Immune Escape in Lung Adenocarcinoma by Regulating PD-L1. Int Arch Allergy Immunol. 2025;186(4):345-57.
24. Liu Y, Wu L, Tong R, Yang F, Yin L, Li M, et al. PD-1/PD-L1 Inhibitors in Cervical Cancer. Front Pharmacol. 2019;10:65.
25. Wang Y, Li G. PD-1/PD-L1 blockade in cervical cancer: current studies and perspectives. Front Med. 2019;13(4):438-50.
26. Chen Y, Zander RA, Wu X, Schauder DM, Kasmani MY, Shen J, et al. BATF regulates progenitor to cytolytic effector CD8(+) T cell transition during chronic viral infection. Nat Immunol. 2021;22(8):996-1007.
27. Wang Y, Xiao X, Kong G, Wen M, Wang G, Ghobrial RM, et al. Genetically targeting the BATF family transcription factors BATF and BATF3 in the mouse abrogates effector T cell activities and enables long-term heart allograft survival. Am J Transplant. 2022;22(2):414-26.
28. Ma J, Zheng B, Goswami S, Meng L, Zhang D, Cao C, et al. PD1(Hi) CD8(+) T cells correlate with exhausted signature and poor clinical outcome in hepatocellular carcinoma. J Immunother Cancer. 2019;7(1):331.
29. Kumar B, Singh A, Basar R, Uprety N, Li Y, Fan H, et al. BATF is a major driver of NK cell epigenetic reprogramming and dysfunction in AML. Sci Transl Med. 2024;16(764):eadp0004.
30. Giunco S, Petrara MR, Zangrossi M, Celeghin A, De Rossi A. Extra-telomeric functions of telomerase in the pathogenesis of Epstein-Barr virus-driven B-cell malignancies and potential therapeutic implications. Infect Agent Cancer. 2018;13:14.
31. Su Z, Yang Z, Xu Y, Chen Y, Yu Q. Apoptosis, autophagy, necroptosis, and cancer metastasis. Mol Cancer. 2015;14:48.
32. Zhang Z, Lin M, Wang J, Yang F, Yang P, Liu Y, et al. Calycosin inhibits breast cancer cell migration and invasion by suppressing EMT via BATF/TGF-β1. Aging (Albany NY). 2021;13(12):16009-23.
33. Chen X, Dong H, Jin L. BATF is involved in the malignant phenotype and epithelial-mesenchymal transition of colon cancer cells via ERK/PD-L1 signaling. Histol Histopathol. 2024:18823.
34. Liu X, Zhou W, Zheng D, Yang X, Qing Y, Liao W, et al. BATF-Activated AIM2 Mediates Immune Escape in Lung Adenocarcinoma by Regulating PD-L1. Int Arch Allergy Immunol. 2024:1-13.
35. Liu Q, Ou Q, Shen L, Qiu C, Zhang B, Zhang W, et al. BATF Potentially Mediates Negative Regulation of PD-1/PD-Ls Pathway on T Cell Functions in Mycobacterium tuberculosis Infection. Front Immunol. 2019;10:2430.
36. Koch S, Sopel N, Finotto S. Th9 and other IL-9-producing cells in allergic asthma. Semin Immunopathol. 2017;39(1):55-68.
37. Jiang F, Wang XY, Wang MY, Mao Y, Miao XL, Wu CY, et al. An Immune Checkpoint-Related Gene Signature for Predicting Survival of Pediatric Acute Myeloid Leukemia. J Oncol. 2021;2021:5550116.
38. Moreno-Villanueva M, Zhang Y, Feiveson A, Mistretta B, Pan Y, Chatterjee S, et al. Single-Cell RNA-Sequencing Identifies Activation of TP53 and STAT1 Pathways in Human T Lymphocyte Subpopulations in Response to Ex Vivo Radiation Exposure. Int J Mol Sci. 2019;20(9).
39. Fujita H, Asahina A, Tada Y, Fujiwara H, Tamaki K. Type I interferons inhibit maturation and activation of mouse Langerhans cells. J Invest Dermatol. 2005;125(1):126-33.